A well-balanced numerical scheme for the approximation of the shallow-water equations with topography: the resonance phenomenon

Ashwin Chinnayya[†]

[†] *CORIA, UMR CNRS 6614, Université de Rouen, Site Universitaire du Madrillet BP12, 76801 Saint-Etienne du Rouvray cedex, France*

Ashwin.Chinnayya@coria.fr

Alain-Yves LeRoux[⋆]

[⋆] *LaBAG/IMB UFR Mathématiques, Université de Bordeaux I, 33400 Talence, France*

Alain-Yves.Leroux@math.u-bordeaux.fr

Nicolas Seguin[‡]

[‡] *ISITV, Avenue George Pompidou, BP 56, 83162 La Valette du Var cedex, France*

seguin@univ-tln.fr

Abstract

The shallow water model with a source term due to topography gradient is approximated within the frame of Finite Volume numerical methods. The cornerstone of the method is the solution of the inhomogeneous Riemann problem. Thus the numerical scheme can deal simultaneously with discrete steady states, flood, occurrence and covering of dry zones. We present the parameterization through the discontinuity of topography, emphasizing on the resonance phenomenon. We then build the solution of the inhomogeneous Riemann problem using a *continuation* method with respect to the jump of topography. Finally, numerical experiments illustrate the agreement of the numerical method with the previous analysis.

Key words : shallow-water equations, source term, well-balanced numerical scheme, resonance.

1 Introduction

The design of numerical methods for the shallow water model in the frame of Finite Volume numerical schemes deserves attention [EGH00].

The shallow-water equations model a free surface flow of incompressible water, over a non flat topography [dSV71, Sto92]. This model is often used to simulate river, coastal flows and dam-break flood. The two-dimensional system of partial differential equations (PDE) writes

$$\frac{\partial h}{\partial t} + \frac{\partial hu}{\partial x} = 0, \tag{1a}$$

$$\frac{\partial (hu)}{\partial t} + \frac{\partial (hu^2)}{\partial x} + \frac{\partial (huv)}{\partial y} + g\frac{\partial}{\partial x}\Big(\frac{h^2}{2}\Big) = -gh\frac{\partial a}{\partial x}, \tag{1b}$$

$$\frac{\partial (hv)}{\partial t} + \frac{\partial (huv)}{\partial x} + \frac{\partial (hv^2)}{\partial y} + g\frac{\partial}{\partial y}\Big(\frac{h^2}{2}\Big) = -gh\frac{\partial a}{\partial y}, \tag{1c}$$

where h, u and v are three functions of time $t \in \mathbb{R}_+$ and space $(x, y) \in \mathbb{R}^2$. These variables denote respectively the vertical height of the water (from the bottom to the surface of the water), the first and the second coordinate of the horizontal velocity. The function a is the vertical height of the topography, from an arbitrary level of reference, $h + a$ is the height of the free surface from this level and g is the gravity constant. The topography a is a function of the space $(x, y) \in \mathbb{R}^2$. When the topography a is assumed to be smooth, that is $a \in \mathcal{C}^0(\mathbb{R}^2)$, the analysis of (1) is straightforward. The left hand-side of the system is strictly hyperbolic while the right hand-side is a classical geometric source term. One of the purposes of the paper is to provide a solution in a particular case of discontinuous topography: a represents a step meaning a is a Heaviside function. This situation can appear when water passes above a dam during a flood.

The problem of the approximation of this system of PDE is difficult. First of all, this includes all the usual difficulties which are due to the discretization of hyperbolic systems of conservation laws when source term is zero. The design of entropy satisfying discrete solutions is widely documented (see for instance [GR96]). The complexity of the problem increases when the source term PDE is non-zero. The time step must follow constraints in order to explicit numerical methods for hyperbolic problems to be stable. If the characteristic time step of the source term is much smaller than the characteristic time step of the convective part of the equations, the overall problem is said to be stiff. The classical numerical methods, such as the *splitting* method, may provide erroneous physical solutions on coarse meshes.

The second problem concerns the positivity of the height of water h. Computations with the shallow-water model involve almost all the time dry zones (wherein $h = hu = hv = 0$) which must be handled by the numerical method. Classical methods lead to a loss of conservation of the height of water or to an infinitely small time step.

The third feature of a numerical method is its capability of preserving stationary solutions. Consider a non-flat topography a and an initial datum which fulfils $h + a \equiv \text{Cst}$ and $(u, v) \equiv (0, 0)$ (like a lake at rest). This datum is a stationary solution of the system (1). The numerical method must preserve such invariant,

that is the numerical method should not make the stationary solution evolve and propagate waves. The numerical model should include intrinsically the variation of the topography in its derivation in order to verify this property. For example, the well-known *splitting* method gives birth to numerical perturbations for this test case, as shown by LeRoux [LeR98]. Besides, in some cases of variations of smooth/great topography gradients, classical numerical methods can give rise to local non pressure loss which are non-physical solutions.

Numerous numerical methods have already been proposed for (1) and the reader is referred to [Bou02] for a large overview of numerical schemes for hyperbolic systems with source terms (see also [GHS03, KL02, LeV98, PS01]).

In this paper, a Finite Volume numerical scheme that has the following properties is presented. The numerical scheme is entropy satisfying. It belongs to the upwind methods. One can show the positivity of the discrete height of water in one-dimensional simulation for a classical CFL (Courant-Friedrichs-Lewy) condition on the time step: time step restriction based only on the convective part. Finally, it can handle any jump of topography and preserves discrete stationary states such as states at rest, like a lake, and hydraulic jumps. Thus it is a good candidate to solve the problems occurring during numerical simulations listed above. This numerical method is an extension of the Godunov's numerical scheme [God59] to inhomogeneous equations. The first reference about this numerical scheme may be found in [IT95] and, in an independent work, Greenberg and LeRoux [GL96b] called this method *the well-balanced numerical scheme*. As in many numerical methods, the topography is approximated by a piecewise constant function within each cell of the mesh. Therefore, between two neighboring cells, the topography is no longer smooth: a discontinuity occurs at the interface. The numerical formalism transforms a smooth topography into a piecewise constant function. The well-balanced numerical scheme is based on the exact solution of the Riemann problem computed with this discontinuity of topography as an initial condition.

In the particular case of the prototype scalar equation $u_t + f(u)_x = g(u)a'(x)$, a smooth enough, Isaacson and Temple show in [IT95] the convergence of this numerical scheme to the entropy solution. But this result has not been extended to systems of PDE. The system of PDE we consider with the initial conditions of the Riemann problem is nonstrictly hyperbolic and nonconservative [DLM95, LeF89]. For a certain set of data, Goatin and LeFloch [GL03] have listed up to three solutions. Indeed, the solution of this kind of system of PDE involves some specific features related to the resonance phenomenon: two eigenvalues of the propagation matrix collapse (see section 3 for further details). In the case of shallow water model with non flat topography, resonance appears when the speed of one of the gravity waves vanishes. We will show that the non-uniqueness can happen under great topography gradient and sudden change of flow regime from torrential (supersonic) to fluvial (subsonic) flow. Our method of parameterization being equivalent to the one proposed in [GL03], the uniqueness of the solution cannot be achieved. With the help of a *continuation* method with respect to the jump of topography and fine numerical simulation, the solution embedded into the Riemann solver is justified.

The second section recalls the Godunov's numerical scheme for one-dimensional homogeneous hyperbolic systems. Then the well-balanced numerical scheme is pre-

sented. The main properties of the numerical scheme are given, based on properties of the solution of the Riemann problem.

The third section gives the main guidelines to solve the Riemann problem, which is the core of the well-balanced numerical method. Let us emphasize that we do not present the complete construction of the solution [Seg99], but the main tools to build it. The main purpose of this section is to study the behavior of the solutions through the *standing wave*, with or without resonance through the discontinuity of topography. Pertaining to the complete construction of the solution of the Riemann problem, the *continuation* method with respect to the jump of topography which is proposed enables the classification of the different kinds of wave patterns coming from the waves being not ordered. This method illustrates this difficulty by four solutions of the Riemann problem with a discontinuous topography and by a case where the solution of the Riemann problem is not unique.

The fourth section corresponds to the numerical simulations provided by the well-balanced numerical scheme that corresponds to the latter analysis. This illustrates the continuation method and how the increase of the jump of topography changes the wave pattern.

2 The well-balanced numerical scheme

The Godunov's numerical scheme [God59] is presented for systems of conservation laws. The well-balanced numerical scheme [GL96b] which is an extension of the Godunov's numerical scheme for hyperbolic systems with source terms is presented afterwards. For simplicity, we restrict the presentation to the one-dimensional framework. The system (1) then reads

$$\frac{\partial \mathbf{u}}{\partial t} + \frac{\partial \mathbf{f}(\mathbf{u})}{\partial x} = \mathbf{s}(\mathbf{u})a'(x),$$

with $\mathbf{u} = {}^T(h, hu)$, the flux function $\mathbf{f}(\mathbf{u}) = {}^T(hu, hu^2 + gh^2/2)$ and the source term $\mathbf{s}(\mathbf{u}) = {}^T(0, -gh)$. This system is complemented with the following initial condition

$$\mathbf{u}(t = 0, x) = \mathbf{u}_0(x), \quad \forall x \in \mathbb{R}. \tag{2}$$

We assume that the mesh is regular, keeping in mind that this method can be extended easily to unstructured meshes. The sequence $(x_{i+1/2})_{i\in\mathbb{Z}}$ is defined such that $x_{i+1/2} = x_{i-1/2} + \Delta x$, Δx being the space step. Furthermore, the sequence $(t^n)_{n\in\mathbb{N}}$ is defined such that $t^0 = 0$, $t^{n+1} = t^n + \Delta t$ and Δt is the temporal increment.

2.1 The Godunov's numerical scheme for systems of conservation laws

Assume the source term to be zero: $a'(x) = 0$. Then the system of PDE to approximate can be written under the conservation form

$$\frac{\partial \mathbf{u}}{\partial t} + \frac{\partial \mathbf{f}(\mathbf{u})}{\partial x} = 0. \tag{3}$$

The solution $\mathbf{u}$ of the Cauchy problem (3)-(2) is approximated by the discrete values $\mathbf{u}_i^n$, $i \in \mathbb{Z}$, $n \in \mathbb{N}$,

$$\mathbf{u}_i^0 = \frac{1}{\Delta x}\int_{x_{i-1/2}}^{x_{i+1/2}} \mathbf{u}_0(x)\,\mathrm{d}x \quad \text{and} \quad \mathbf{u}_i^n = \frac{1}{\Delta x}\int_{x_{i-1/2}}^{x_{i+1/2}} \mathbf{u}(t^n,x)\,\mathrm{d}x. \tag{4}$$

The Godunov's numerical scheme is the result of the Green's formula applied to the integral of system (3) over $(t^n;t^{n+1})\times(x_{i-1/2};x_{i+1/2})$

$$\int_{t^n}^{t^{n+1}}\int_{x_{i-1/2}}^{x_{i+1/2}} \left(\frac{\partial \mathbf{u}}{\partial t} + \frac{\partial \mathbf{f}(\mathbf{u})}{\partial x}\right)\mathrm{d}x\,\mathrm{d}t = 0,$$

which yields

$$\begin{aligned}\int_{x_{i-1/2}}^{x_{i+1/2}} (\mathbf{u}(t^{n+1},x) - \mathbf{u}(t^n,x))\,\mathrm{d}x \\ + \int_{t^n}^{t^{n+1}} (\mathbf{f}(\mathbf{u}(t,x_{i+1/2}^-)) - \mathbf{f}(\mathbf{u}(t,x_{i-1/2}^+)))\,\mathrm{d}t = 0,\end{aligned} \tag{5}$$

where x^- and x^+ respectively denote the left-hand and right-hand limits of x. Such a precision is needed because the solution $\mathbf{u}$ can be discontinuous through the interfaces parallel to the axis $x=0$ (but, due to the hyperbolicity, the discontinuities cannot be parallel to the axis $t=0$). The first integral of (5) is approximated using (4). It remains to define the numerical approximations of the flux.

Since, at each time step, the approximate solution initially is a piecewise function constant over each cell, the computation of $\mathbf{u}(t,x_{i+1/2}^-)$ and $\mathbf{u}(t,x_{i+1/2}^+)$ for $t \in (t^n;t^{n+1})$ is given by the solution of the following Riemann problem

$$\begin{cases} \dfrac{\partial \mathbf{u}}{\partial t} + \dfrac{\partial \mathbf{f}(\mathbf{u})}{\partial x} = 0, \quad t \in (t^n;t^{n+1}),\ x \in \mathbb{R}, \\ \mathbf{u}(t^n,x) = \begin{cases} \mathbf{u}_i^n & \text{if } x < x_{i+1/2} \\ \mathbf{u}_{i+1}^n & \text{if } x > x_{i+1/2} \end{cases}. \end{cases} \tag{6}$$

Let us note $\mathbf{u}_{i+1/2}^n(x/t;\mathbf{u}_i^n,\mathbf{u}_{i+1}^n)$ its self-similar solution. Due to the system (3) to be conservative, the equality

$$\mathbf{f}(\mathbf{u}_{i+1/2}^n(0^-;\mathbf{u}_i^n,\mathbf{u}_{i+1}^n)) = \mathbf{f}(\mathbf{u}_{i+1/2}^n(0^+;\mathbf{u}_i^n,\mathbf{u}_{i+1}^n)) \tag{7}$$

holds. Therefore, we define the numerical flux $\mathbf{f}_{i+1/2}^n$ by

$$\mathbf{f}_{i+1/2}^n = \mathbf{f}(\mathbf{u}_{i+1/2}^n(0^-;\mathbf{u}_i^n,\mathbf{u}_{i+1}^n)) = \mathbf{f}(\mathbf{u}_{i+1/2}^n(0^+;\mathbf{u}_i^n,\mathbf{u}_{i+1}^n)). \tag{8}$$

The Godunov's numerical scheme is thus defined by

$$\mathbf{u}_i^{n+1} = \mathbf{u}_i^n - \frac{\Delta t}{\Delta x}\big(\mathbf{f}_{i+1/2}^n - \mathbf{f}_{i-1/2}^n\big), \tag{9}$$

with the numerical flux (8). In order to ensure the stability of the numerical scheme, a CFL condition is needed. It limits the time step Δt in function of the space step

Δx and the maximal wave speed of each local Riemann problem λ_M. This time step restriction corresponds to the non-interaction of the waves of each local Riemann problem

$$\Delta t \leq \frac{\Delta x}{2\,\lambda_M}. \tag{10}$$

The continuity of the numerical flux (8) comes from the system (3) to be conservative. This property no longer holds with nonconservative systems. The following section deals with such characteristic.

2.2 The well-balanced numerical scheme for inhomogeneous systems

The one-dimensional counterpart of system (1) can be written under the form

$$\frac{\partial \mathbf{u}}{\partial t} + \frac{\partial \mathbf{f}(\mathbf{u})}{\partial x} = \mathbf{s}(\mathbf{u})a'(x). \tag{11}$$

The difficulty here is the approximation of the source term $\mathbf{s}(\mathbf{u})a'(x)$. Indeed, if the slope of topography $a'(x)$ is great, the source term becomes stiff and it has to be carefully approximated to the numerical scheme to be stable. The idea developed in [IT95] and [GL96b] in the scalar case is adapted to the system (11).

First, let a_Δ be the approximation of a:

$$a_i = \frac{1}{\Delta x}\int_{x_{i-1/2}}^{x_{i+1/2}} a(x)\,\mathrm{d}x \quad \text{and} \quad a_\Delta(x) = \sum_{i\in\mathbb{Z}} a_i\chi_i(x), \tag{12}$$

where $\chi_i(x) = 1$ if $x \in (x_{i-1/2}; x_{i+1/2})$ and $\chi_i(x) = 0$ elsewhere. The approximate topography a_Δ is considered as an additional "unknown" and the system (11) is then approximated by the nonconservative system

$$\frac{\partial a_\Delta}{\partial t} = 0, \tag{13a}$$

$$\frac{\partial \mathbf{u}}{\partial t} + \frac{\partial \mathbf{f}(\mathbf{u})}{\partial x} - \mathbf{s}(\mathbf{u})\frac{\partial a_\Delta}{\partial x} = 0. \tag{13b}$$

The convex Lax entropy pair associated with this nonconservative system is

$$(\eta, F_\eta)(a_\Delta, \mathbf{u}) = (hu^2/2 + gh^2/2 + gha_\Delta, hu(u^2/2 + g(h + a_\Delta))). \tag{14}$$

The well-balanced numerical scheme is obtained following the same process as in the previous section 2.1. The first step is the integration of (13b) over $(t^n; t^{n+1}) \times (x_{i-1/2}; x_{i+1/2})$. Since in this domain $\partial_x a_\Delta = 0$, we obtain once again

$$\int_{t^n}^{t^{n+1}}\int_{x_{i-1/2}}^{x_{i+1/2}} \left(\frac{\partial \mathbf{u}}{\partial t} + \frac{\partial \mathbf{f}(\mathbf{u})}{\partial x}\right)\,\mathrm{d}x\,\mathrm{d}t = 0.$$

Applying the Green's formula yields (5) again. As above, the first integral is approximated using (4). Due to the nonconservation of (13), the continuity of the flux (7) does not hold anymore. Two numerical fluxes have to be defined for each

interface $\mathbf{f}^{n,-}_{i+1/2}$ and $\mathbf{f}^{n,+}_{i+1/2}$. They are computed with the help of the solution of the local Riemann problem

$$\left\{\begin{array}{l} \dfrac{\partial a_\Delta}{\partial t} = 0, \\ \dfrac{\partial \mathbf{u}}{\partial t} + \dfrac{\partial \mathbf{f}(\mathbf{u})}{\partial x} - \mathbf{s}(\mathbf{u})\dfrac{\partial a_\Delta}{\partial x} = 0, \quad t \in (t^n; t^{n+1}),\ x \in \mathbb{R}, \\ \mathbf{u}(t^n, x) = \begin{cases} \mathbf{u}^n_i & \text{if } x < x_{i+1/2} \\ \mathbf{u}^n_{i+1} & \text{if } x > x_{i+1/2} \end{cases} \quad \text{and} \quad a_\Delta(x) = \begin{cases} a_i & \text{if } x < x_{i+1/2} \\ a_{i+1} & \text{if } x > x_{i+1/2} \end{cases}. \end{array}\right. \tag{15}$$

If we denote by $\mathbf{u}^n_{i+1/2}(x/t; \mathbf{u}^n_i, \mathbf{u}^n_{i+1})$ its self-similar solution, the numerical fluxes are defined by

$$\mathbf{f}^{n,-}_{i+1/2} = \mathbf{f}\big(\mathbf{u}^n_{i+1/2}(0^-; \mathbf{u}^n_i, \mathbf{u}^n_{i+1})\big) \quad \text{and} \quad \mathbf{f}^{n,+}_{i+1/2} = \mathbf{f}\big(\mathbf{u}^n_{i+1/2}(0^+; \mathbf{u}^n_i, \mathbf{u}^n_{i+1})\big), \tag{16}$$

and the corresponding numerical scheme is

$$\mathbf{u}^{n+1}_i = \mathbf{u}^n_i - \frac{\Delta t}{\Delta x}\big(\mathbf{f}^{n,-}_{i+1/2} - \mathbf{f}^{n,+}_{i-1/2}\big). \tag{17}$$

Note that, in general, $\mathbf{f}^{n,-}_{i+1/2} \neq \mathbf{f}^{n,+}_{i+1/2}$.

This numerical scheme is called the well-balanced numerical scheme. Of course, the method must be complemented by the CFL condition (10) to ensure its stability.

The construction of the well-balanced numerical scheme is very similar to the construction of the Godunov's numerical scheme and they share several properties listed below.

Proposition 2.1 *We note $\mathbf{u}^0_{\Delta x}(x)$ the piecewise constant function defined by $\mathbf{u}^0_i$ in cell $(x_{i-1/2}; x_{i+1/2})$. We assume that the corresponding height of water $h^0_{\Delta x}(x)$ is nonnegative for all $x \in \mathbb{R}$ and that the solution of the Riemann problems* (15) *exists in the set of nonnegative height of water. Then, the well-balanced numerical scheme, under the CFL condition* (10)*, fulfils the following properties*

1. *$h^n_i \geq 0$, $\forall n \in \mathbb{N}$, $\forall i \in \mathbb{Z}$,*
2. *it is entropy satisfying with respect to the entropy pair* (14)*,*
3. *if we assume that the solution $\mathbf{u}$ of the system* (13) *with the initial condition*

$$\mathbf{u}(t = 0, x) = \mathbf{u}^0_{\Delta x}(x), \quad \forall x \in \mathbb{R},$$

is stationary (ie $\partial_t \mathbf{u} = 0$, $\forall (t, x) \in \mathbb{R}_+ \times \mathbb{R}$), then, the well-balanced numerical scheme (16)-(17) *ensures that*

$$\mathbf{u}^n_i = \mathbf{u}^0_i, \quad \forall n \in \mathbb{N}, \forall i \in \mathbb{Z}.$$

Proof The well-balanced numerical scheme can be interpreted as a *convection-L^2 projection* algorithm since it is built on the same principles as the Godunov's numerical scheme (see [GR96]). This interpretation makes easier the proof of the three properties.

1. Since the solution of the Riemann problems (15) is supposed to provide nonnegative heights of water, the *convection* step provides on the whole space domain a nonnegative height of water. Besides, the L^2 *projection* on the space mesh preserves the positivity of the height of water. Since $h^0_{\Delta x}(x) \geq 0 \; \forall x \in \mathbb{R}$, the property 1 holds.

2. Of course, in the *convection* step, the rate of entropy dissipation decreases. In the L^2 *projection* step, arguing that the entropy η is convex and using the Jensen's inequality, the rate of entropy dissipation decreases (see [CP98] and [Tad86] for more details).

3. It is clear that, since the initial datum $\mathbf{u}^0_{\Delta x}$ is stationary, the *convection* step preserves it. Moreover, it is piecewise constant on each cell of the mesh, then it is also preserved by the L^2 *projection* step. □

As mentioned in the introduction, the global construction of the solution of the Riemann problem for the system (13) is not presented here (refer to [Seg99] instead). Thus we assume that the solution of the Riemann problem exists and has a nonnegative height of water.

The third result is very important in the frame of the shallow-water model. Indeed, stationary solutions often occur in simulations: flow at rest ($h+a \equiv cste$, $u \equiv 0$), stationary hydraulic jumps ($hu \equiv cste$, $hu^2 + gh^2/2 \equiv cste$), stationary smooth flows ($hu \equiv cste$, $u^2/2 + g(h+a) \equiv cste$). To the best of the authors' knowledge, the well-balanced numerical scheme is the unique numerical scheme which verifies this property. Pertaining to the scalar version of the well-balanced scheme, refer to [Gos98, GL96a, GL96b, IT95].

At this stage, the last ingredient to define completely the well-balanced numerical scheme is the construction of the solution of the Riemann problem (15).

3 The Riemann problem

The aim of this section is to provide the main guidelines to solve the following Riemann problem

$$\left\{ \begin{array}{l} \dfrac{\partial a_\Delta}{\partial t} = 0, \\ \dfrac{\partial \mathbf{u}}{\partial t} + \dfrac{\partial \mathbf{f}(\mathbf{u})}{\partial x} - \mathbf{s}(\mathbf{u}) \dfrac{\partial a_\Delta}{\partial x} = 0, \quad t \in \mathbb{R}^*_+, \, x \in \mathbb{R}, \\ \mathbf{u}(t^n, x) = \begin{cases} \mathbf{u}_L & \text{if } x < 0 \\ \mathbf{u}_R & \text{if } x > 0 \end{cases} \quad \text{and} \quad a_\Delta(x) = \begin{cases} a_L & \text{if } x < 0 \\ a_R & \text{if } x > 0 \end{cases}. \end{array} \right. \tag{18}$$

The system (13) can be written for smooth solutions as

$$\frac{\partial}{\partial t} \begin{pmatrix} a_\Delta \\ \mathbf{u} \end{pmatrix} + \mathbf{A}(\mathbf{u}) \frac{\partial}{\partial x} \begin{pmatrix} a_\Delta \\ \mathbf{u} \end{pmatrix} = 0, \text{ with } \mathbf{A}(\mathbf{u}) = \begin{pmatrix} 0 & 0 \\ -\mathbf{s}(\mathbf{u}) & \mathbf{Df}(\mathbf{u}) \end{pmatrix}.$$

A straightforward analysis of $\mathbf{A}(\mathbf{u})$ provides that this system is nonstrictly hyperbolic, which means that the eigenvalues of $\mathbf{A}(\mathbf{u})$ are always real, but, for some values of $\mathbf{u}$, the eigenvectors of $\mathbf{A}(\mathbf{u})$ are not linearly independent. In the following, the 1-wave is associated with the eigenvalue of $A(\mathbf{u})$ $\lambda_1(\mathbf{u}) = u - c$ and the 2-wave is associated with the eigenvalue $\lambda_2(\mathbf{u}) = u + c$, with $c = \sqrt{gh}$ the speed of gravity

waves. These two waves correspond to genuinely non linear fields and, therefore, are rarefaction waves or shock waves. The third eigenvalue of $\mathbf{A}(\mathbf{u})$ is $\lambda_0(\mathbf{u}) = 0$ and corresponds to a linearly degenerate field (this 0-wave is thus a contact discontinuity). In fact, the matrix $\mathbf{A}(\mathbf{u})$ is not diagonalizable if and only if $|u| = \sqrt{gh}$, that is when the 1-wave or the 2-wave is superposed with the 0-wave. This is called in the literature the *resonance* phenomenon.

This system is nonconservative and the definition of discontinuous solutions can be ambiguous [DLM95, LeF89]. In the domains $D^- = \{t \geq 0, x < 0\}$ and $D^+ = \{t \geq 0, x > 0\}$, a_Δ is constant and the system (13) is locally conservative and strictly hyperbolic. The difficulty is thus located at $\{t > 0; x = 0\}$, assuming obviously that $a_L \neq a_R$. Since the field associated with the 0-wave is linearly degenerate, the Rankine-Hugoniot jump relations through the 0-wave can be defined using the 0-Riemann invariants, when $|u| \neq \sqrt{gh}$. In the *resonant* case, that is when the solution locally complies with $|u| = \sqrt{gh}$, since a genuinely non linear field (that is the wave $u - c$ or $u + c$) is superposed with the linearly degenerate field (that is the 0-wave), the 0-Riemann invariants cannot be used to parameterize the solution through the discontinuity at $x = 0$. A deeper analysis is thus required.

Let us begin with the parameterization of the 1-wave and of the 2-wave in the non resonant case.

3.1 The parameterisation of the gravity waves

The parameterization of the 1-wave and of the 2-wave is classical when their speed is non-zero since the topography is locally flat and, thus, the source term locally vanishes. Then, in order to connect a state $\mathbf{u}$ to another state $\mathbf{u}_0$ through a gravity wave, we use the standard Riemann invariants and Rankine-Hugoniot jump relations.

To connect (from the left to the right) a state $\mathbf{u}$ to a state $\mathbf{u}_0$ through the 1-wave $u - c$, one may use the following relation (a rarefaction wave occurs when $h < h_0$, and a shock wave occurs when $h > h_0$)

$$u = \begin{cases} u_0 - 2(\sqrt{gh} - \sqrt{gh_0}) & \text{if } h < h_0, \\ u_0 - (h - h_0)\sqrt{g\dfrac{h + h_0}{2hh_0}} & \text{if } h > h_0. \end{cases} \tag{19}$$

In the same way, to connect (from the right to the left) a state $\mathbf{u}$ to a state $\mathbf{u}_0$ through the 2-wave $u + c$, one may use the following relation (a rarefaction wave occurs when $h < h_0$, and a shock wave occurs when $h > h_0$)

$$u = \begin{cases} u_0 + 2(\sqrt{gh} - \sqrt{gh_0}) & \text{if } h < h_0, \\ u_0 + (h - h_0)\sqrt{g\dfrac{h + h_0}{2hh_0}} & \text{if } h > h_0. \end{cases} \tag{20}$$

Besides, the speed of propagation σ of a 1 or 2-shock wave is given by

$$\sigma = \frac{hu - h_0u_0}{h - h_0}. \tag{21}$$

We focus now on the behavior of the solution of (18) through the discontinuity of topography, with or without resonance.

3.2 The parameterization through the discontinuity of topography

At least in the non resonant case, the solution should be described using the 0-Riemann invariants, since this discontinuity corresponds to a linearly degenerate field. The 0-Riemann invariants write

$$I_0^1(a,\mathbf{u}) = hu \quad \text{and} \quad I_0^2(a,\mathbf{u}) = \frac{u^2}{2} + g(h+a). \tag{22}$$

Then, if $\mathbf{u}_l$ and $\mathbf{u}_r$ denote the states located at the left and at the right of $\{x=0\}$, the system

$$I_0^1(a_L,\mathbf{u}_l) = I_0^1(a_R,\mathbf{u}_r), \quad I_0^2(a_L,\mathbf{u}_l) = I_0^2(a_R,\mathbf{u}_r),$$

assuming that $\mathbf{u}_l$, a_L and a_R are given, admits zero, one or two solutions $\mathbf{u}_r$. It is clear that a deeper analysis must be performed, at least to select one solution when two are admissible.

In [LeR98], an original approach has been proposed to describe, more precisely than simply using the 0-Riemann invariants, the behaviour of the solution through the discontinuity, in the frame of the shallow water model with topography. This is based on a geometric regularization of the discontinuity of topography. More recently, Goatin and LeFloch [GL03] described the solution for a general set of resonant inhomogeneous systems (involving the shallow water with topography), using an arbitrary parameter which smoothly links the states $(a_L,\mathbf{u}_l)$ and $(a_R,\mathbf{u}_r)$. These two approaches are equivalent (see remark 1). Here, the approach at first proposed by LeRoux (see also [Seg99, CL99], [Col92]) is detailed. It has also been used in [SV03] in the frame of a resonant conservation law for proving the existence and the uniqueness of the associated entropy weak solution.

We are interested in the wave of speed 0. The solution of (18) through the discontinuity $\{x=0\}$ is self-similar. We assume that a_L, $\mathbf{u}_l = \mathbf{u}(x/t=0^-)$ and a_R are given. We choose to parameterize the solution with respect to x. To achieve this purpose, the interface is thickened, that is the discontinuous topography is replaced by a continuous topography $a_\varepsilon(x)$ for $x \in [-\varepsilon;+\varepsilon]$, $\varepsilon > 0$, which verifies

- $a_\varepsilon(x \le -\varepsilon) = a_L$ and $a_\varepsilon(x \ge \varepsilon) = a_R$,
- $\operatorname{sign}(a_\varepsilon'(x)) = \operatorname{sign}(a_R - a_L)$, for all $x \in (-\varepsilon;+\varepsilon)$.

Then we seek the solutions $(h_\varepsilon, h_\varepsilon u_\varepsilon)(x) \in \mathbb{R}_+ \times \mathbb{R}$ of the nonlinear system

$$\frac{\mathrm{d}}{\mathrm{d}x}(h_\varepsilon u_\varepsilon) = 0, \qquad x \in (-\varepsilon;+\varepsilon), \tag{23a}$$

$$\frac{\mathrm{d}}{\mathrm{d}x}\left(h_\varepsilon u_\varepsilon^2 + g\frac{h_\varepsilon^2}{2}\right) = -gh_\varepsilon\frac{\mathrm{d}a_\varepsilon}{\mathrm{d}x}, \qquad x \in (-\varepsilon;+\varepsilon), \tag{23b}$$

with the boundary condition

$$(h_\varepsilon, h_\varepsilon u_\varepsilon)(-\varepsilon) = (h_l, Q_l), \tag{23c}$$

where $h_l > 0$ and $Q_l \in \mathbb{R}$. One may check that the structure of the solutions of (23) is preserved when ε tends to zero.

In the following, we denote the flow rate $Q_\varepsilon = h_\varepsilon u_\varepsilon$. The problem (23) may be ill-posed. Nonetheless, if we note $(h_r, h_r u_r) = (h_\varepsilon, h_\varepsilon u_\varepsilon)(+\varepsilon)$, the knowledge of the admissible pair(s) $(h_r, h_r u_r)$ for a given pair (h_l, Q_l) will describe the behavior of the solution through stationary waves at $\{x = 0\}$ and to construct the solution of (18).

We are interested in the piecewise smooth solutions of (23). The following is devoted to the study of the smooth solutions of (23) and the admissible discontinuities associated with (23). These discontinuities are stationary 1-shock waves or stationary 2-shock waves of the system (13) and the denominations "discontinuity" and "stationary shock" will be used indifferently. Their admissibility is led by the entropy criterion: the Lax inequalities are used. When ε tends to zero, these discontinuities correspond to stationary shock waves located at $x = 0$.

First of all, we provide the solution of (23) when considering a zero discharge Q_l. In this case, the solution in the frame of piecewise smooth functions is explicit and is based on the fact that $(0, 0)$ is a solution of the system (23a)-(23b).

Proposition 3.1 *Assume that $Q_l = 0$. Then, the unique piecewise smooth solution of problem* (23) *in $\mathbb{R}_+ \times \mathbb{R}$ is*

$$h_\varepsilon(x) = \max(h_l + a_L - a_\varepsilon(x), 0), \tag{24}$$

$$Q_\varepsilon(x) = 0, \tag{25}$$

for $x \in [-\varepsilon; \varepsilon]$.

Proof Equation (23a), in the sense of distributions, immediately provides that $Q_\varepsilon \equiv 0$, that is (25). Let us turn now to h_ε. In smooth parts,

$$g h_\varepsilon \frac{\mathrm{d}}{\mathrm{d}x}(h_\varepsilon + a_\varepsilon) = 0 \tag{26}$$

holds. Then either $h_\varepsilon = 0$ or $\mathrm{d}_x(h_\varepsilon + a_\varepsilon) = 0$ in the smooth parts of the solution. Besides the Rankine-Hugoniot jump relation associated with (23b) gives

$$\frac{1}{2}\big((h^+)^2 - (h^-)^2\big) = 0,$$

where the superscripts $^-$ and $^+$ refer to the states at the left and the right of the stationary shock. We obtain that $\mathbf{u}^- = \mathbf{u}^+$ and that the solution is continuous. Therefore the unique continuous solution $h_\varepsilon(x) \in \mathbb{R}_+$ which verifies (26) is (24). □

The following part is devoted to the smooth solutions of (23) assuming that Q_l is non-zero. Their behaviour will be detailed and will be useful for constructing not only smooth solutions of (23) (that is a pure 0-wave, without resonance) but also to describe the smooth parts of the solution when it involves discontinuities.

3.2.1 Smooth solutions of (23) for a non-zero discharge

Restricting to smooth solutions of (23), the system (23a)-(23b) is written under the following conservative form

$$\begin{array}{l} \dfrac{\mathrm{d}}{\mathrm{d}x}(h_\varepsilon u_\varepsilon) = 0, \\ \dfrac{\mathrm{d}}{\mathrm{d}x}\left(\dfrac{u_\varepsilon^2}{2} + g(h_\varepsilon + a_\varepsilon)\right) = 0. \end{array} \tag{27}$$

One recognizes here the 0-Riemann invariants (22).

Definition 3.2 *Let us introduce the following sets:*

- $\mathcal{T} = \{(h, hu) \in \mathbb{R}_+^* \times \mathbb{R}; |u| > \sqrt{gh}\}$, *which represents the set of the* torrential *states, also described as* supercritical *states;*
- $\mathcal{F} = \{(h, hu) \in \mathbb{R}_+^* \times \mathbb{R}; |u| < \sqrt{gh}\}$, *which represents the set of the* fluvial *states, also described as* subcritical *states;*
- $\mathcal{C} = \{(h, hu) \in \mathbb{R}_+^* \times \mathbb{R}; |u| = \sqrt{gh}\}$, *which represents the set of the* critical *states.*

It follows that $\mathbb{R}_+^* \times \mathbb{R} = \mathcal{T} \cup \mathcal{F} \cup \mathcal{C}$.

This classification is the same as the classification of supersonic, subsonic and sonic flows in aeronautics. It will allow us to describe some important features of the solution $(h_\varepsilon, h_\varepsilon u_\varepsilon)$. We now define the function ψ as

$$\begin{array}{l} \mathbb{R}_+^* \times \mathbb{R} \longmapsto \mathbb{R}_+ \\ \quad (h, Q) \longmapsto \psi(h, Q) = \dfrac{Q^2}{2h^2} + gh. \end{array} \tag{28}$$

As the solution $(h_\varepsilon, h_\varepsilon u_\varepsilon)$ will be expressed with the help of ψ, some information about this function is needed.

Lemma 3.3 *For a given Q, the function $\psi(\,.\,, Q)$ verifies the following properties:*

1. *this function is strictly convex;*
2. *it has a (global) minimum at $h_m = \frac{Q^{2/3}}{g^{1/3}}$ and (h_m, Q) belongs to the set of critical states $\mathcal{C}$;*
3. *let h_0 be a positive constant such that $\psi(h_0, Q) > \psi(h_m, Q)$. Then, if $h_0 < h_m$, the pair (h_0, Q) lies in $\mathcal{T}$ while if $h_0 > h_m$, the pair (h_0, Q) lies in $\mathcal{F}$.*

The proof of these properties is straightforward.

The function ψ enables a new formulation of the problem (23):

Lemma 3.4 *A pair $(h_\varepsilon, Q_\varepsilon)$ is a smooth solution of problem (23) if and only if it is a smooth solution of*

$$\psi(h_\varepsilon(x), Q_l) = \psi(h_l, Q_l) - g(a_\varepsilon(x) - a_L), \quad x \in [-\varepsilon; +\varepsilon], \tag{29a}$$

$$Q_\varepsilon(x) = Q_l, \tag{29b}$$

with the boundary condition

$$h_\varepsilon(-\varepsilon) = h_l. \tag{29c}$$

This simple result is obtained by integration of system (27) over $(-\varepsilon; x)$ and by the Green's formula.

The height of water h_ε is given by the implicit equation (29a) and the velocity u_ε is deduced from (29b). At this stage, the description of the smooth solutions of (23) provided until now is strictly the same as the description which would have been obtained using the 0-Riemann invariants. As mentioned above, (29a) may provide zero, one or two solutions $h_\varepsilon(\varepsilon)$, due to the behavior of ψ described in lemma 3.3, and the number of solutions depends on the right hand-side of (29a). It is rather unsatisfying, but a deeper analysis will provide more information. Let us study the behavior of the solution of (29) according to the sign of $a_\varepsilon(x) - a_L$ that is the sign of $a_R - a_L$.

The decreasing slope case We consider here that $a_L > a_R$. In such a configuration, equation (29a) becomes $\psi(h_\varepsilon(x), Q_l) > \psi(h_l, Q_l)$. Since $\psi(h_l, Q_l) \geq \psi(h_m, Q_l)$, the third item of lemma 3.3 ensures that equation (29a) always admits two distinct solutions for $x = +\varepsilon$, denoted h_r^- and h_r^+, such that

$$0 < h_r^- < h_m(Q_l) < h_r^+.$$

For the sake of simplicity, we denote from now h_m instead of $h_m(Q_l)$. The following result can be stated.

Proposition 3.5 *Assume that $a_L > a_R$. If $(h_l, Q_l) \in \mathcal{T}$ (respectively $(h_l, Q_l) \in \mathcal{F}$), there exists one and only one smooth solution $(h_\varepsilon, Q_\varepsilon)$ of the problem (23). Moreover, for all $x \in [-\varepsilon; +\varepsilon]$, we have $(h_\varepsilon, Q_\varepsilon)(x) \in \mathcal{T}$ (resp. $(h_\varepsilon, Q_\varepsilon)(x) \in \mathcal{F}$).*
If $(h_l, Q_l) \in \mathcal{C}$, then two smooth solutions are admissible: the one in $\mathcal{T}$ and the other in $\mathcal{F}$.

Proof We consider the derivative of equation (29a) with respect to x,

$$\frac{\mathrm{d}}{\mathrm{d}x}\big(\psi(h_\varepsilon(x), Q_l)\big) = -g\, a'_\varepsilon(x)$$

i.e.

$$\frac{\partial \psi}{\partial h}(h_\varepsilon, Q_l)\, h'_\varepsilon(x) = -g\, a'_\varepsilon(x).$$

Due to the assumption on the slope of topography, this equation becomes

$$\frac{\partial \psi}{\partial h}(h_\varepsilon, Q_l)\, h'_\varepsilon(x) > 0. \tag{30}$$

This inequality provide an additional information about the solution of (23). We obtain the following classification (see also figure 1):

- Assume first that $h_\varepsilon(-\varepsilon) = h_l < h_m$ (that is $(h_l, Q_l) \in \mathcal{T}$). Let us recall the requirements that h_ε must fulfil: $h_\varepsilon(-\varepsilon) = h_l$, h_ε is smooth and inequality (30). It is straightforward to check that the unique solution h_ε of (29a) is such that $h'_\varepsilon(x) < 0$, for all $x \in (-\varepsilon; +\varepsilon)$ and, therefore, $h_\varepsilon(\varepsilon) = h_r^- < h_l$. Notice that, in this case, the corresponding solution of (29) belongs to $\mathcal{T}$.

- Consider now that $h_l > h_m$. Using once again inequality (30), the solution of (29) belongs to $\mathcal{F}$ and $h_\varepsilon(\varepsilon) = h_r^+ > h_l$.

- If $h_l = h_m$, then the problem (23) admits two different solutions h_ε^- and h_ε^+, such that $(h_\varepsilon^-)'(x) < 0$ and $(h_\varepsilon^+)'(x) > 0$, for $x \in (-\varepsilon; +\varepsilon)$. They respectively take the value h_r^- and h_r^+ for $x = +\varepsilon$.

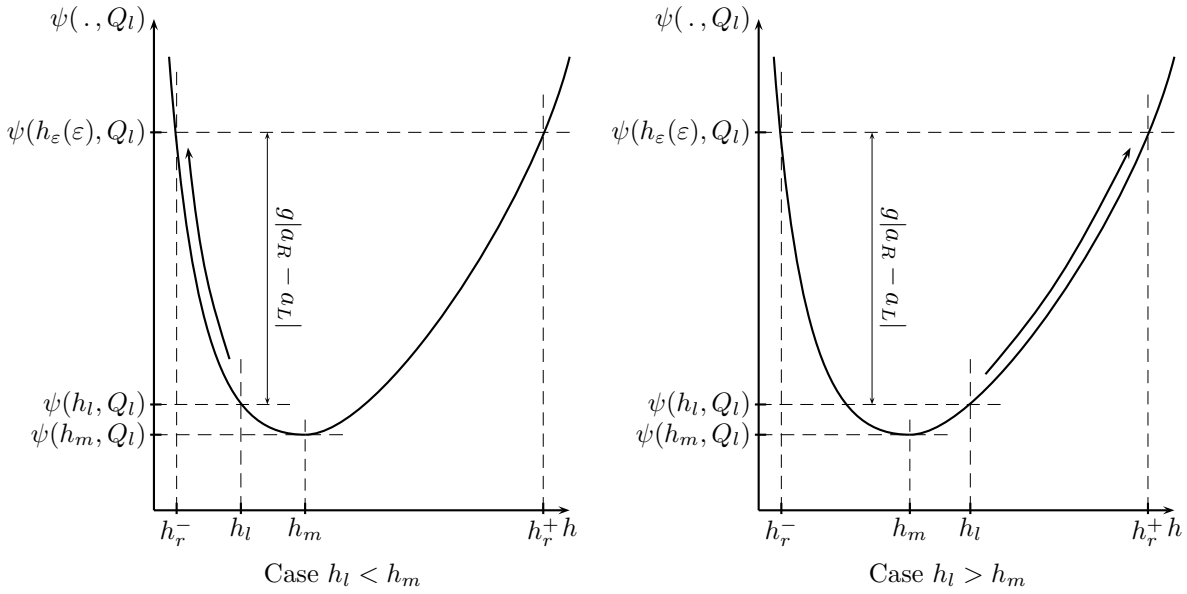

Figure 1: Smooth solutions of the equation (29a), with $a_L > a_R$.

□

The increasing slope case We focus herein on the case $a_L < a_R$. The configuration is slightly different. Indeed, for some data, equation (29a) may admit no smooth solution. Such a result is not in contradiction with the existence of a solution of (18), it simply means that the boundary condition (23c) is not relevant (refer to [SV03] where the same phenomenon is described in a more simple frame). Indeed, the boundary condition (23c) can be modified by introducing a 1-wave for instance with a negative speed, such that the intermediate state provide a suitable boundary condition (23c), for which the equation (29a) admits a solution.

More precisely, we state the following result:

Proposition 3.6 *Assume that $a_L < a_R$. If $\psi(h_l, Q_l) - g(a_R - a_L) < \psi(h_m, Q_l)$, the problem* (23) *admits no solution.*

Nonetheless, if $\psi(h_l, Q_l) - g(a_R - a_L) \geq \psi(h_m, Q_l)$*, there exists one and only one smooth solution* $(h_\varepsilon, Q_\varepsilon)$ *of the problem* (23)*. As above, if* $(h_l, Q_l) \in \mathcal{T}$ *(respectively* $(h_l, Q_l) \in \mathcal{F}$*), the solution* $(h_\varepsilon, Q_\varepsilon)(x)$ *belongs to* $\mathcal{T} \cup \mathcal{C}$ *(resp.* $\mathcal{F} \cup \mathcal{C}$*) for all* $x \in [-\varepsilon; +\varepsilon]$*.*

Proof The nonexistence result is straightforward, when considering equation (29a) and lemma 3.3.

Now, let us consider the case $\psi(h_l, Q_l) - g(a_R - a_L) \geq \psi(h_m, Q_l)$. Once more, two solutions are available. The derivative of equation (29a) with respect to x and the assumption on the slope of topography gives

$$\frac{\partial \psi}{\partial h}(h_\varepsilon, Q_l)\, h'_\varepsilon(x) < 0, \quad \forall x \in (-\varepsilon; +\varepsilon). \tag{31}$$

The same process as in the case $a_L > a_R$ provides the following classification (see also figure 2):

- If $h_l < h_m$, equation (31) implies that $h'_\varepsilon(x)$ is non-negative for $x \in (-\varepsilon; +\varepsilon)$. It follows that the solution h_ε is unique and takes the value h_r^- for $x = +\varepsilon$. Remark that $h_l < h_r^- \leq h_m$.
- Assuming now that $h_l > h_m$, one may obtain with the help of (31) that $h'_\varepsilon(x)$ is non-positive for $x \in (-\varepsilon; +\varepsilon)$. The solution h_ε is unique and it takes the value h_r^+ for $x = +\varepsilon$. In this case, we have $h_m \leq h_r^+ < h_l$.

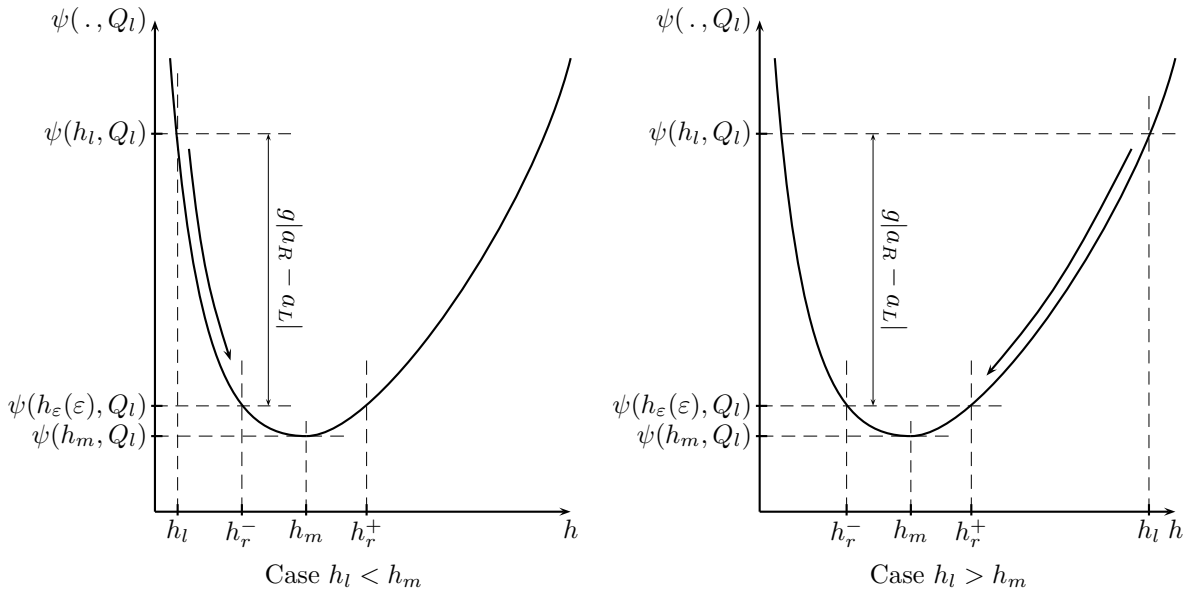

Figure 2: Smooth solutions of the equation (29a), with $a_L < a_R$.

□

3.2.2 Admissible discontinuities for (23) with a non-zero discharge

Let x_0 be the position of a discontinuity in $[-\varepsilon;+\varepsilon]$, and $\mathbf{u}^-$ and $\mathbf{u}^+$ ($\neq \mathbf{u}^-$) the states respectively located at the left and at the right of the discontinuity. A discontinuity for the system (23) corresponds to a stationary shock wave of the system (13). Therefore, we complement the definition of a discontinuity by an entropy criterion: the Lax inequalities.

Since the topography a_ε is smooth, the Rankine-Hugoniot jump relations are

$$Q^+ - Q^- = 0, \tag{32a}$$

$$\left(h^+(u^+)^2 + g\frac{(h^+)^2}{2}\right) - \left(h^-(u^-)^2 + g\frac{(h^-)^2}{2}\right) = 0. \tag{32b}$$

With the help of these relations, it is straightforward to see that the assumption $\mathbf{u}^+ \neq \mathbf{u}^-$ ensures that $Q^- = Q^+ \neq 0$. This discontinuity must verify the Lax inequalities

$$\lambda(\mathbf{u}^-) > 0 > \lambda(\mathbf{u}^+), \tag{33}$$

where 0 is the speed of the discontinuity. When the discontinuity corresponds to a stationary 1-shock wave for system (13), $\lambda(\mathbf{u}) = u - c$ and if it corresponds to a stationary 2-shock wave, $\lambda(\mathbf{u}) = u + c$.

Proposition 3.7 *If the states $\mathbf{u}^-$ and $\mathbf{u}^+$ ($\neq \mathbf{u}^-$) are separated by a discontinuity that corresponds to a stationary 1-shock wave (respectively to a stationary 2-shock wave) for (13), then $\mathbf{u}^-$ lies in $\mathcal{T}$ (resp. in $\mathcal{F}$) and $\mathbf{u}^+$ lies in $\mathcal{F}$ (resp. in $\mathcal{T}$).*

Proof First of all, let us define the function ϕ

$$\begin{aligned} \mathbb{R}_+^* \times \mathbb{R} &\longmapsto \mathbb{R}_+ \\ (h, Q) &\longmapsto \phi(h, Q) = \frac{Q^2}{h} + g\frac{h^2}{2}. \end{aligned} \tag{34}$$

The function $\phi(., Q)$ has the same behavior as $\psi(., Q)$ for a given Q (see lemma 3.3), that is

- this function is strictly convex;
- it has a (global) minimum at $h_m = \frac{Q^{2/3}}{g^{1/3}}$ and $(h_m, Q) \in \mathcal{C}$;
- let h_0 be a positive constant such that $\phi(h_0, Q) > \phi(h_m, Q)$. Then, if $h_0 < h_m$, the pair (h_0, Q) lies in $\mathcal{T}$ while if $h_0 > h_m$, the pair (h_0, Q) lies in $\mathcal{F}$.

Therefore, using this function, the Rankine-Hugoniot jump relations (32) become

$$\begin{aligned} Q^- &= Q^+, \\ \phi(h^-, Q^-) &= \phi(h^+, Q^-). \end{aligned}$$

Since $\mathbf{u}^- \neq \mathbf{u}^+$, the third item ensures that if $\mathbf{u}^- \in \mathcal{T}$, then $\mathbf{u}^+ \in \mathcal{F}$, and, conversely, if $\mathbf{u}^- \in \mathcal{F}$, then $\mathbf{u}^+ \in \mathcal{T}$.

Let us now assume that $\mathbf{u}^- \in \mathcal{F}$ is separated from $\mathbf{u}^+ \in \mathcal{T}$ by a discontinuity corresponding to a stationary 1-shock wave for (13). The Lax entropy condition (33) then writes

$$u^- - c^- > 0 > u^+ - c^+.$$

The first inequality gives $u^- > c^-$, which is in contradiction with $\mathbf{u}^- \in \mathcal{F}$. Therefore, for a stationary 1-shock wave, we have $\mathbf{u}^- \in \mathcal{T}$ and $\mathbf{u}^+ \in \mathcal{F}$. The case of a 2-shock wave is handled in the same way. □

Note that this result is well-known, at least in the frame of gas dynamics in a duct [AW04, LT03]. Furthermore, this proposition has an immediate consequence:

Corollary 3.8 *Assume that the entropy weak solution* $(h_\varepsilon, Q_\varepsilon)$ *of problem* (23) *is composed by smooth parts separated by admissible discontinuities in the sense of* (33) *and that* $Q_l \neq 0$. *Therefore, the solution admits* at most one *discontinuity in* $[-\varepsilon; +\varepsilon]$.

Proof As mentioned previously, this discontinuity is a stationary 1 or 2-shock wave. Since $h_l > 0$, it is clear from propositions 3.5, 3.6 and 3.7 that $h_\varepsilon(x) \neq 0$, for all $x \in [-\varepsilon; +\varepsilon]$. Then, a solution of (23) cannot admit a stationary 1-shock wave and a stationary 2-shock wave at the same time. Furthermore, a smooth part of a solution cannot cross the set $\mathcal{C}$. Hencefore, using proposition 3.7, a solution of (23) composed by smooth parts separated by a stationary 1-shock wave must have the form

- from $-\varepsilon$ to x_0: $(h_\varepsilon, Q_\varepsilon)$ is smooth and lies in $\mathcal{T}$;
- in x_0: $(h_\varepsilon, Q_\varepsilon)$ admits a stationary 1-shock wave;
- from x_0 to $+\varepsilon$: $(h_\varepsilon, Q_\varepsilon)$ is smooth and lies in $\mathcal{F}$.

We proceed in the same way for solutions of (23) composed by smooth parts separated by stationary 2-shock wave:

- from $-\varepsilon$ to x_0: $(h_\varepsilon, Q_\varepsilon)$ is smooth and lies in $\mathcal{F}$;
- in x_0: $(h_\varepsilon, Q_\varepsilon)$ admits a stationary 2-shock wave;
- from x_0 to $+\varepsilon$: $(h_\varepsilon, Q_\varepsilon)$ is smooth and lies in $\mathcal{T}$.

□

Remark 1 We chose here to parameterize the behavior of the solution through the discontinuity of topography with respect to x, thickening the interface. One can prove that all the previous results can be obtained by just parameterizing the pair $(a, \mathbf{u})$ *with respect to a variable, say* $\mu \in [0; 1]$, *such that* $a(\mu = 0) = a_L$, $a(\mu = 1) = a_R$ *and* $sign(a'(\mu)) = sign(a_R - a_L)$ *(instead of x varying from* $-\varepsilon$ *to* $+\varepsilon$*). Such a formulation corresponds to the ones used in [Vas02, GL03].*

Remark 2 Moreover, the dependence of $(h_\varepsilon, Q_\varepsilon)$ *is only due to* $a_\varepsilon(x)$ *(see lemma 3.4). As a consequence, one shows that, if a solution obtained with the regularization involves a discontinuity, the position* x_0 *of the discontinuity depends on the*

value of $a_\varepsilon(x_0)$. In other words, if a discontinuity occurs at x_0^1 for a regularization a_ε^1, then, for a distinct regularization a_ε^2, this discontinuity will be located at $x_0^2 = (a_\varepsilon^2)^{-1}(a_\varepsilon^1(x_0^1))$. Nevertheless, in both cases, the position of this discontinuity tends to 0 as ε tends to zero.

Remark 3 The 0*-Riemann invariants for system* (13) *are*

$$I_0^1(a, \mathbf{u}) = hu \quad \textit{and} \quad I_0^2(a, \mathbf{u}) = \frac{u^2}{2} + g(h + a).$$

If the solution of (23) *is smooth, then $I_0^1(a_L, \mathbf{u}_l) = I_0^1(a_R, \mathbf{u}_r)$ and $I_0^2(a_L, \mathbf{u}_l) = I_0^2(a_R, \mathbf{u}_r)$ hold. But in the case of the presence of a shock wave superposed with $\{x = 0\}$, we have now $I_0^2(a_L, \mathbf{u}_l) \neq I_0^2(a_R, \mathbf{u}_r)$. This is due to the different parameterizations provided by the* 0*-Riemann invariants and the Rankine-Hugoniot jump relations* (32) *(see the example of section 3.3.3). In such a configuration, the solution of the corresponding Riemann is resonant since the speed of the shock wave is zero. The other resonant configuration corresponds to a solution of a Riemann problem such that a rarefaction wave is critical, which means that the speed of one of the bounds of its fan is zero.*

3.3 Some solutions to the Riemann problem

We provide here some tools and examples to solve the Riemann problem (18). This Riemann problem is much more difficult than in the case of a flat bottom. In particular, the three waves are not ordered, which greatly increases the number of wave patterns. Moreover, the parameterization of the 0-wave is not explicit. In order to overcome these numerical difficulties and provide a general Riemann solver for any set of initial data $(a_L, \mathbf{u}_L)$ and $(a_R, \mathbf{u}_R)$, we use a *continuation* method with respect to the difference of topography. The idea in order to solve the Riemann problem (18) is to start with a null jump of topography $|a_R - a_L| = 0$ and let it increase until obtaining the jump of topography required in (18), letting the associated solution vary in a smooth way with respect to $a_R - a_L$. When three solutions of (18) are available, it is worth noting that this method of construction does not enable to select one of these. The non-uniqueness is discussed later, in the section 3.3.5.

Using the relations (19) and (20), $\mathcal{W}_1(\mathbf{u}_0)$ defines the curve defined by the set of states which can be linked to $\mathbf{u}_0$ by a 1-wave, such that $\mathbf{u}_0$ is at the left of the 1-wave and any state $\mathbf{u}_1 \in \mathcal{W}_1(\mathbf{u}_0)$ is at its right, with respect to x. $\mathcal{W}_2(\mathbf{u}_0)$ defines the curve containing all the states which can be linked to $\mathbf{u}_0$ by a 2-wave, such that $\mathbf{u}_0$ is at the right of the 2-wave and any $\mathbf{u}_1 \in \mathcal{W}_2(\mathbf{u}_0)$ is at its left, with respect to x (see section 3.1).

The solution for some initial conditions is exhibited, together with a representation in the phase plane (u, c). The successive initial conditions considered at first are such that $h_L < h_R$ and $u_L = u_R = 0$. The four situations described below correspond to several decreasing steps of topography.

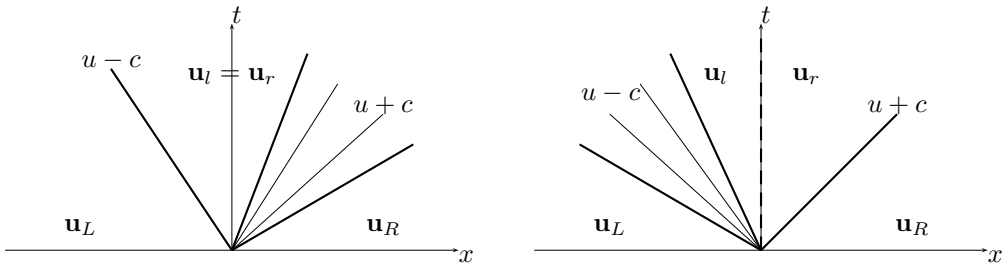

a — No step of topography.

b — A small step of topography.

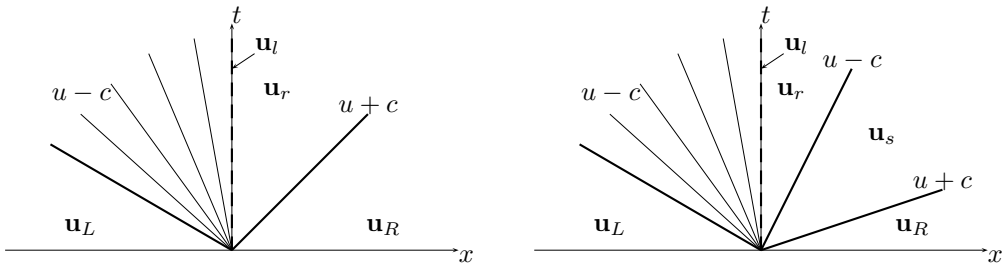

c — A medium step of topography.

d — A large step of topography.

Figure 3: The four solutions in the (x, t)-plane.

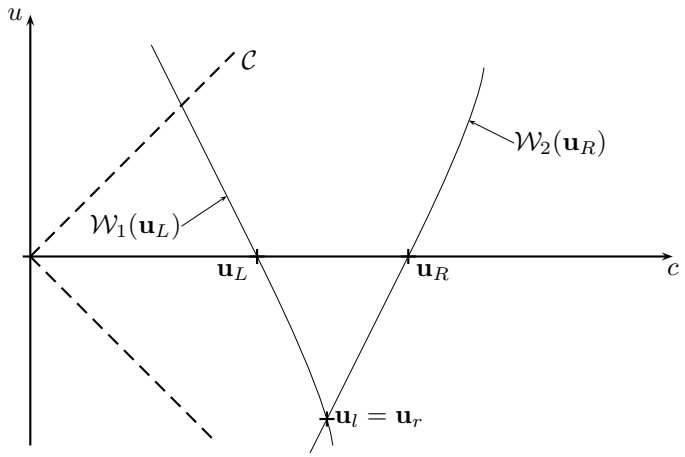

Figure 4: No step of topography.

3.3.1 A solution on a flat topography

In this first configuration, we assume that $a_L = a_R$. It leads to a solution composed by $\mathbf{u}_L$, a 1-shock wave, an intermediate state denoted $\mathbf{u}_l = \mathbf{u}_r$ in figure 4, a 2-rarefaction wave and $\mathbf{u}_R$ (see also figure 3-a). This solution is standard since it corresponds to a strictly hyperbolic conservative system.

3.3.2 A small step of topography

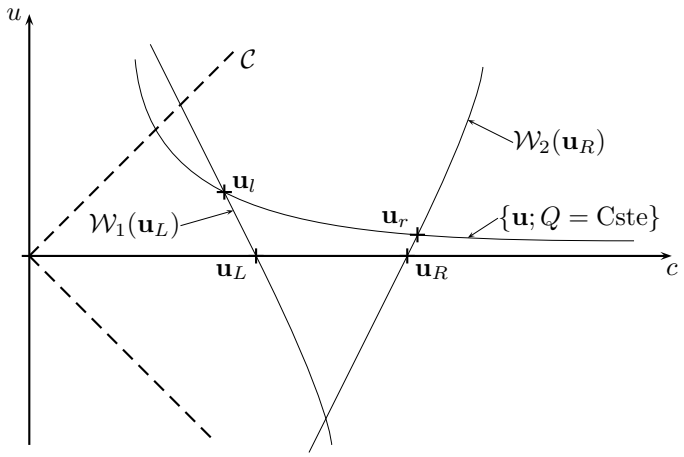

Figure 5: A small step of topography.

In this second situation, we have $a_L > a_R$, such that the solution follows the description in figure 5. The solution becomes obviously more complex than in the previous case. In the domain $\{t > 0, x < 0\}$, the solution is composed by $\mathbf{u}_L$ separated by a 1-rarefaction wave to the state $\mathbf{u}_l$, while in $\{t > 0, x > 0\}$, it is composed by $\mathbf{u}_r$ separated from $\mathbf{u}_R$ by a 2-shock wave (see figure 3-b). Besides, the states $\mathbf{u}_l$ and $\mathbf{u}_r$ comply with the relations $Q_l = Q_r$ and $\psi(h_r, Q_r) - \psi(h_l, Q_l) = -g(a_R - a_L)$, and both $\mathbf{u}_l$ and $\mathbf{u}_r$ belong to $\mathcal{F}$, in agreement with lemma 3.4 and proposition 3.5.

In this case of non-flat topography, the flow rate across the standing wave is positive whereas in the previous case of flat topography, the flow rate was negative. During the *continuation* process, the increase of the jump of topography $|a_L - a_R|$ makes the flow rate increase. Moreover, the 1-wave is now a rarefaction wave whereas in the previous case, it was a shock wave. It does not contradict the smooth variation of the solution with respect to $|a_L - a_R|$, since for the intermediate jump of topography $a_L - a_R = h_R - h_L$, the flow rate is zero and the two genuinely non linear waves have a zero amplitude.

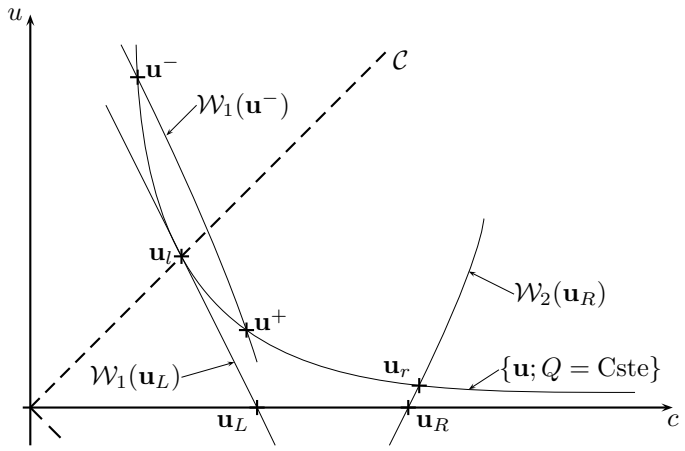

Figure 6: A medium step of topography.

3.3.3 A medium step of topography

We now consider a larger decreasing step of topography, such that a stationary 1-shock wave appears, superposed on the discontinuity of topography. The corresponding solution is depicted in figure 6.

Before commenting this solution, let us go back to the solution of the previous paragraph. As mentioned, this solution verifies $Q_l = Q_r$, $\psi(h_r, Q_r) - \psi(h_l, Q_l) = -g(a_R - a_L)$ and $\mathbf{u}_l, \mathbf{u}_r \in \mathcal{F}$. Now, let the jump of topography $a_L - a_R$ grow, trying to fulfil both relations and setting $\mathbf{u}_l \in \mathcal{W}_1(\mathbf{u}_L)$ and $\mathbf{u}_r \in \mathcal{W}_2(\mathbf{u}_R)$. It is clear that, after a limit value a_m of $a_L - a_R$, some of these requirements become incompatible. Precisely, this limit value is defined by $a_m = (\psi(h_r, Q_r) - \psi(h_l, Q_l))/g$, where $\mathbf{u}_l$ and $\mathbf{u}_r$ are the states represented in figure 6. We then focus here on the case $a_L - a_R > a_m$.

In the domain $\{t > 0, x < 0\}$, the solution built in figure 6 is composed by a 1-rarefaction wave, whose limit speeds are $u_L - c_L$ and $u_l - c_l = 0$. In $\{t > 0, x > 0\}$, the solution is composed by $\mathbf{u}_r$ and $\mathbf{u}_R$, which are linked by a 2-shock wave (see figure 3-c). Let us study now the solution "inside" the interface $\{t > 0, x = 0\}$. The solution is composed by two smooth parts, from $\mathbf{u}_l$ to $\mathbf{u}^-$ and from $\mathbf{u}^+$ to $\mathbf{u}_r$, and $\mathbf{u}^-$ and $\mathbf{u}^+$ are separated by a 1-shock wave. More precisely, these states verify

- the Rankine-Hugoniot jump relations (32) (since $\mathbf{u}^+ \in \mathcal{W}_1(\mathbf{u}^-)$),
- $\mathbf{u}^- \in \mathcal{T}$ and $\mathbf{u}^+ \in \mathcal{F}$ (see proposition 3.7),
- $Q_l = Q^- = Q^+ = Q_r$ and
- $(\psi(h_r, Q_r) - \psi(h^+, Q^+)) + (\psi(h^-, Q^-) - \psi(h_l, Q_l)) = -g(a_R - a_L)$.

These items enable to define uniquely $\mathbf{u}^-$ and $\mathbf{u}^+$. Moreover, the latter item corresponds to a pressure loss through the jump of topography.

All the states of this Riemann problem ($\mathbf{u}_l$, $\mathbf{u}^-$, $\mathbf{u}^+$ and $\mathbf{u}_r$) belong to the same constant flow rate. This flow rate corresponds to the maximal admissible flow rate as the flow is fluvial upstream ($\mathbf{u}_L/c_L < 1$). This solution is well-known in the frame of flows in a nozzle. The 1-rarefaction wave is a sonic rarefaction wave between $\mathbf{u}_L$ and $\mathbf{u}_l$ (see figure 3-c).

3.3.4 A large decreasing step of topography

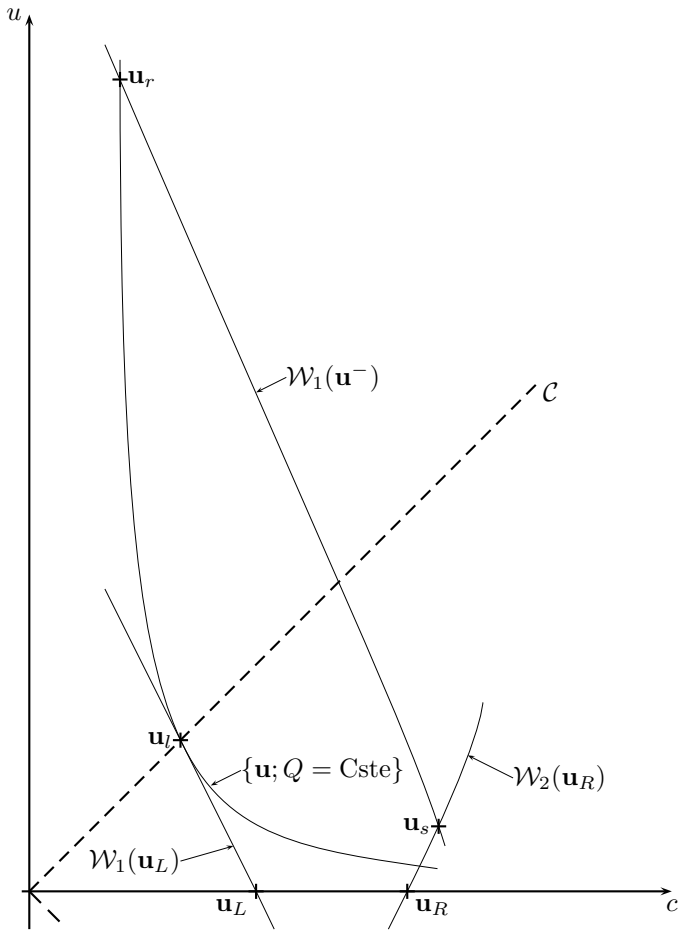

Figure 7: A large step of topography.

We consider now the same initial condition on $\mathbf{u}$ but with, once again, a larger jump $a_L - a_R$ of topography.

Let us define a_M the jump of topography such that the states $\mathbf{u}^+$ and $\mathbf{u}_r$ of the previous example join. More precisely, $a_M = (\psi(h_M^-, Q_M^-) - \psi(h_l, Q_l))/g$, where $\mathbf{u}_M^-$ is such that $Q_M^- = Q_l$ and $\mathbf{u}_r \in \mathcal{W}_1(\mathbf{u}_M^-)$. Still focusing on the previous example, one proves that, letting grow $a_L - a_R$ from a_m to a_M, the stationary 1-shock wave "moves" inside the discontinuity $\{t > 0, x = 0\}$. If we consider the thickening $(-\varepsilon; \varepsilon)$

of the interface, the position of the stationary 1-shock wave evolves from $-\varepsilon$ to $+\varepsilon$ as the jump of topography increases from a_m to a_M. And $\mathbf{u}^+$ varies from $\mathbf{u}_l$ to $\mathbf{u}_r$ in a monotone way in the curve $\{\mathbf{u} : Q = Q_l\}$. Therefore, we consider here that $a_L - a_R > a_M$, which implies that the 1-shock wave of the previous example which was stationary has now a positive velocity.

The solution is still composed in $\{t > 0, x < 0\}$ by a sonic 1-rarefaction wave between $\mathbf{u}_L$ and $\mathbf{u}_l$. In $\{t > 0, x > 0\}$, the solution is respectively composed, from $x = 0$ to $x = +\infty$, by a constant state $\mathbf{u}_r$, a 1-shock wave, a constant state $\mathbf{u}_s$, a 2-shock wave and $\mathbf{u}_R$ (see figure 3-d). It is worth noting that field associated with the first eigenvalue is composed by a 1-rarefaction wave, a constant state and a 1-shock wave.

In some sense, the 1-rarefaction wave $\lambda_1 = u - c$ splits into several components and becomes a composite wave.

3.3.5 A case with three different entropy solutions

The solution of the four latter cases is unique. Here, we study a case where three entropy solutions are available [GL03]. The initial condition is

	$x < 0$	$x > 0$
$a(x)$	0.0	0.1
$h(t = 0, x)$	1.0	1.72626
$Q(t = 0, x)$	$\sqrt{g} + 2.$	$\sqrt{g} + 2.$

with $g = 9.81$. The approximate value $h_R = 1.72626$ has been computed in order to build a stationary solution such that a stationary 1-shock wave is located at $x = 0$ and such that, if we thicken the interface and regularize the topography, it is located at the point $x_0 \in (-\varepsilon; \varepsilon)$ which verifies $a_\varepsilon(x_0) = 0.05$.

As proved in [GL03], this initial datum provides three different solutions:

A - the first one (solid line in the figure (8)) is obviously the stationary solution which has been used to compute h_R and is composed inside $x = 0$ by a smooth part from a_L to $a_0 = 0.05$, with a stationary 1-shock wave located at $a_0 = 0.05$, followed by another smooth part from $a_0 = 0.05$ to a_R;

B - the second one (dotted line in the figure (8)) is composed by a left-going 1-shock wave, with a pure 0-contact discontinuity and a right-going 2-shock wave;

C - the last one (dashed line in the figure (8)) is composed by a pure 0-contact discontinuity, with a right-going 1-shock wave followed by a right-going 2-rarefaction wave.

In this case, the solution which is implemented in the Riemann solver is the second one (see [Seg99]). It is also the second solution which is computed by the whole well-balanced numerical scheme when using this test case as an initial condition in a one-dimensional domain. The solution of the Riemann problem has been chosen in an empiric way based on the supposed intrinsic regularization of the well-balanced numerical scheme. In this particular case, this is important as the solution provided

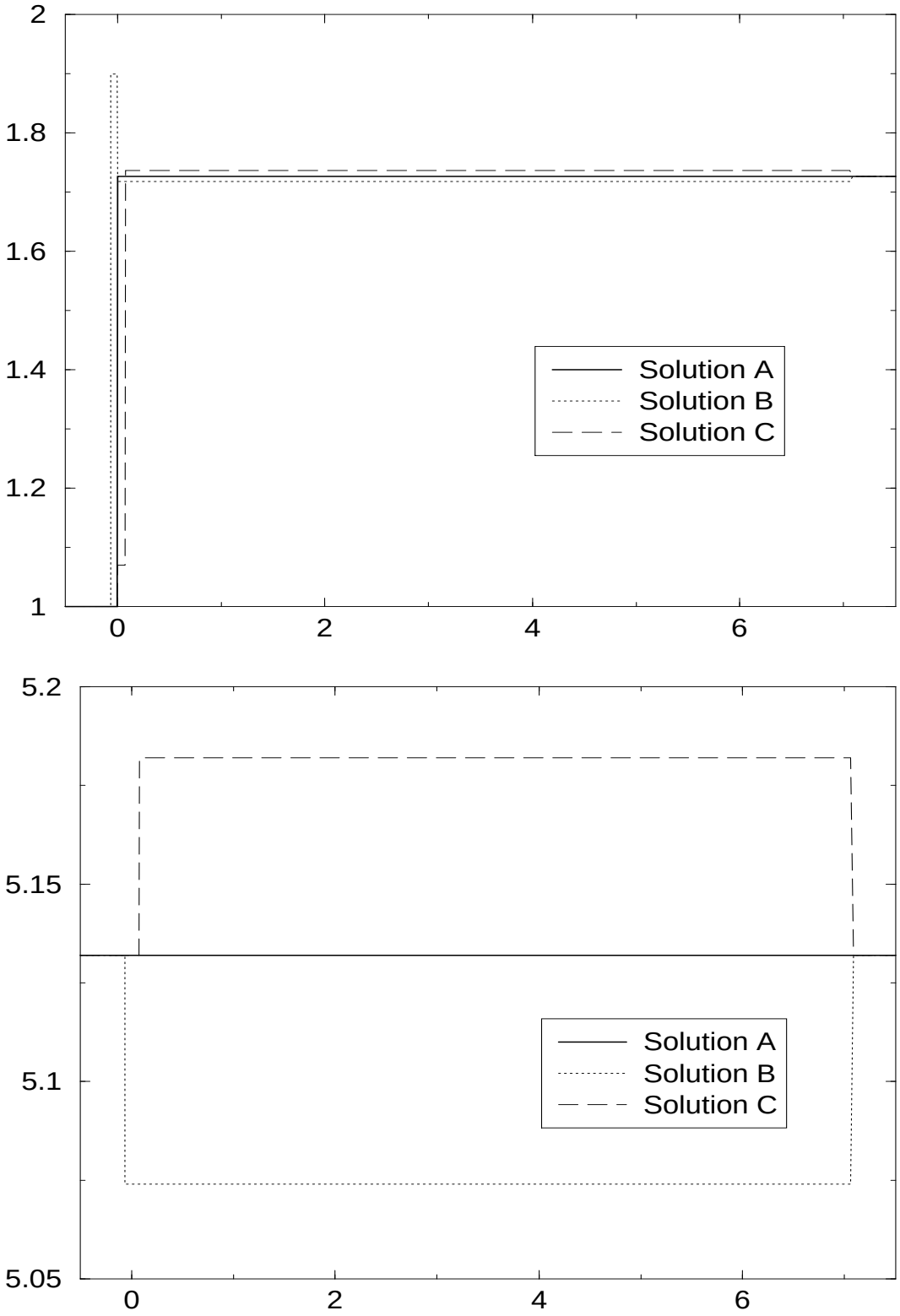

Figure 8: The three exact solutions. Top: h vs x. Bottom: Q vs x.

by the Riemann problem must be coherent with the solution provided by the numerical scheme, in order to prevent numerical oscillations, one historical fundamental basement of the well-balanced numerical scheme.

The problem of non-uniqueness in the resonant nonconservative framework deserves some comments. Up to now and to the best of the authors' knowledge, no criterion has been proposed to select one of these three solutions as well in the scalar case as for systems. Note that, for the shallow-water equations with topography, the three solutions can only occur when the 1-wave interacts with an increasing step of topography and, conversely, when the 2-wave interacts with an decreasing step of topography (see [GL03]).

We now proceed in representative numerical tests that illustrate our matter.

4 Numerical results

Several numerical tests using the well-balanced numerical scheme (16)-(17) for system (13) are presented. These tests correspond to the Riemann problems studied in the previous section. In our simulations, the length of the domain is 25 m, the final time is $1,2$ s and the initial condition is

	$0 \leq x < 12.5$	$12.5 < x \leq 25$
$h(t=0,x)$	3.	4.
$Q(t=0,x)$	0.	0.

(35)

The only datum we modify is the jump of topography. As above, we will make the jump of topography grow and comment the associated solution. All test cases are computed with one thousand cells and the CFL condition used and which is defined on the cells interface, is 0.4.

In all the phase plane figures, the set $\mathcal{C}$ that is $u = \pm c$ and the curve $u = 0$ (zero flow rate) are plotted.

4.1 A test with a flat topography

This first test is quite classical and refers to the solution depicted in figure 4, that is, setting $a(x) = 0$, for $0 \leq x \leq 25$. One may notice in figure 9 that, as expected, the solution is smooth through $x = 12.5$.

4.2 A test with a small decreasing jump of topography

In this case, the topography is $a(x) = 2$ for $0 \leq x \leq 12.5$ and $a(x) = 0$ for $12.5 \leq x \leq 25$. The height of water is no longer smooth through $x = 12.5$ in figure 10 and we clearly see the 1-rarefaction wave and the 2-shock wave, in agreement with the solution depicted in figure 5. Besides, the numerical approximations of hu and $u^2/2 + g(h + a)$ remain constant through $x = 12.5$ in figure 11.

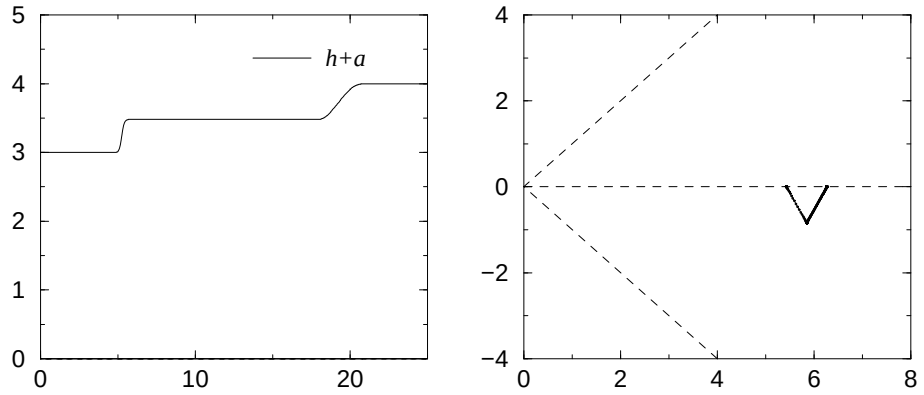

Figure 9: A test with a flat topography. Left: $h + a$ vs x. Right: u vs c.

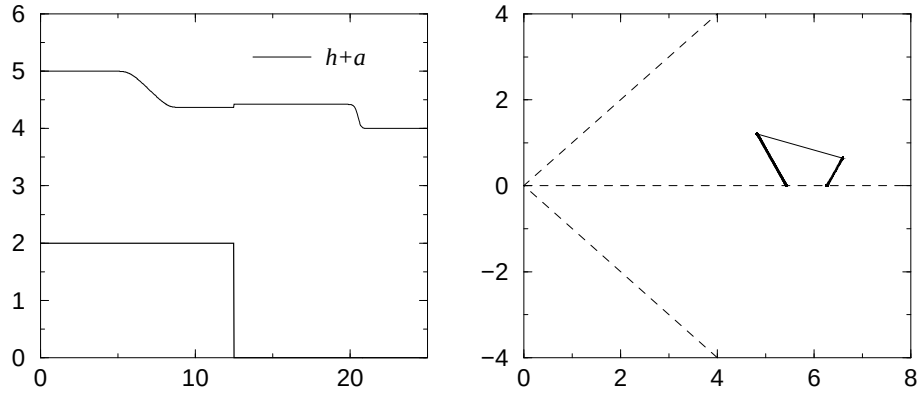

Figure 10: A test with a small decreasing jump of topography. Left: $h + a$ vs x. Right: u vs c.

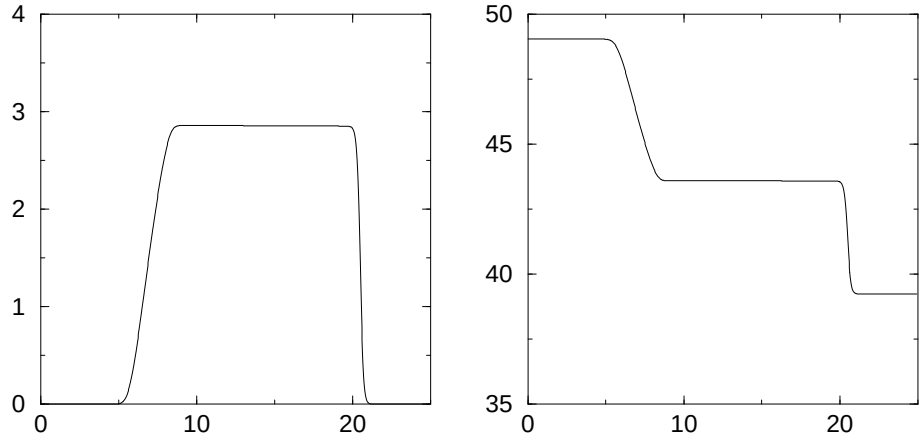

Figure 11: A test with a small decreasing jump of topography. Left: hu vs x. Right: $u^2/2 + g(h + a)$ vs x.

4.3 A test with a stationary 1-shock wave superposed on a decreasing jump of topography

This test corresponds to the solution of figure 6, that is a solution involving a 1-shock wave superposed on the 0-wave. One may see in figure 12 that the 1-rarefaction

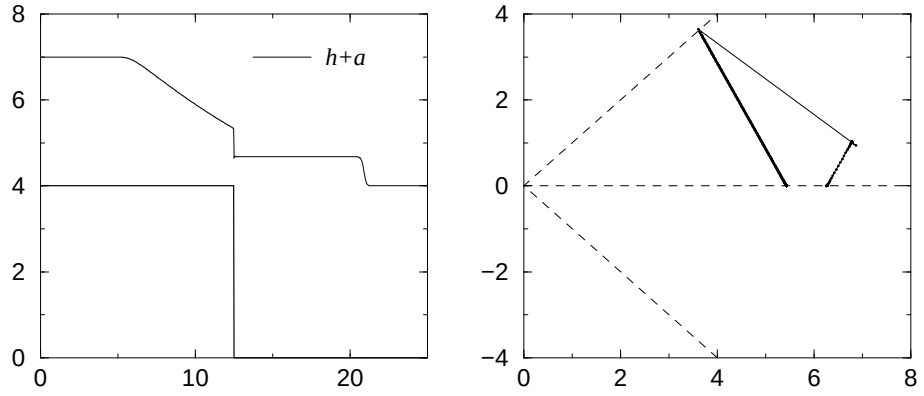

Figure 12: A test with a small decreasing jump of topography. Left: $h + a$ vs x. Right: u vs c.

wave is critical, that is to say $u = c$ at $x = 12.5$. This solution is thus resonant. Besides, when focusing on figure 13-right, one may remark that $u^2/2 + g(h + a)$

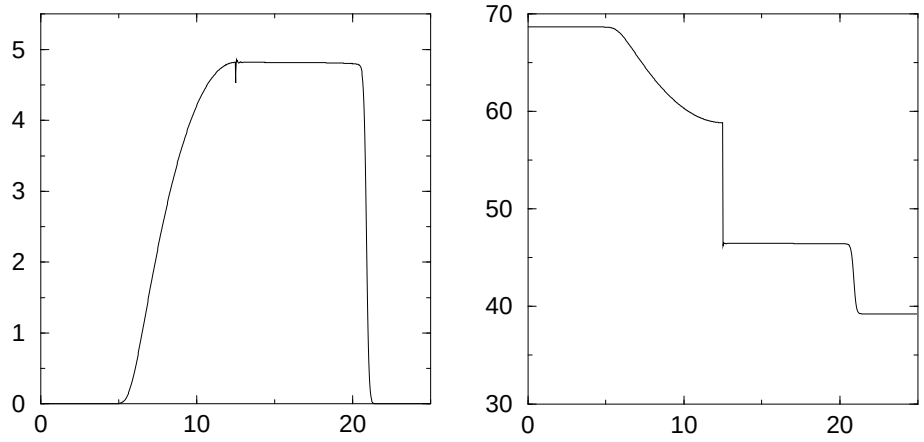

Figure 13: A test with a small decreasing jump of topography. Left: hu vs x. Right: $u^2/2 + g(h + a)$ vs x.

is discontinuous through $x = 12.5$. This is due to the presence of the stationary 1-shock wave which is superposed on the 0-wave. This stationary shock or hydraulic jump induces a pressure loss through the jump of topography.

In order to clarify the presence of this stationary 1-shock wave, an additional

test is provided. In this case, the topography is the following:

$$a(x) = \begin{cases} 4 & 0 \leq x < 25/3, \\ -(12/25)x + 8 & \text{for } 25/3 < x < 50/3, \\ 0 & \text{for } 50/3 < x \leq 25. \end{cases}$$

We set the final time to 6 s (for such a time, the 2-shock wave is out of the domain). In this case, the stationary 1-shock wave clearly appears in figure 14-left (solid

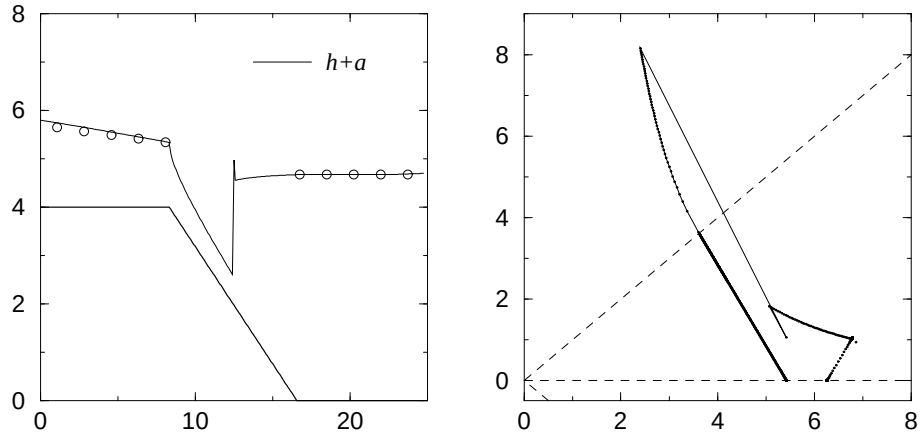

Figure 14: A test with a stationary 1-shock wave over a decreasing slope of topography. Left: $h + a$ vs x. Right: u vs c.

line). Circles represent the results obtained with the same final time, but without regularization, that is to say with a jump of topography (of course, a translation with respect to x has been opered to make both results coincide). We then note the good agreement of the intermediate states with the smooth topography and with a jump of topography.

The figure 14-right represents the result obtained with the regularization of the topography, superposed on the result of the figure 12-right. We then can see the same profile as in figure 6.

4.4 A test with a large decreasing jump of topography

This last test corresponds to figure 7. In this case, the jump of topography is so large that the (previously stationary) 1-shock wave goes out the discontinuity and moves rightwards, with a very slow speed. Note that, as seen in section 3.3.4, the state at the right of the discontinuity of topography verifies $u \gg c$ and corresponds to the upper point in figure 15-right. As we could expect, hu and $u^2/2 + g(h + a)$ remains constant through the jump of topography in figure 16. The oscillations in this figure comes probably from the fact that the speed of the shock is very slow [AR97].

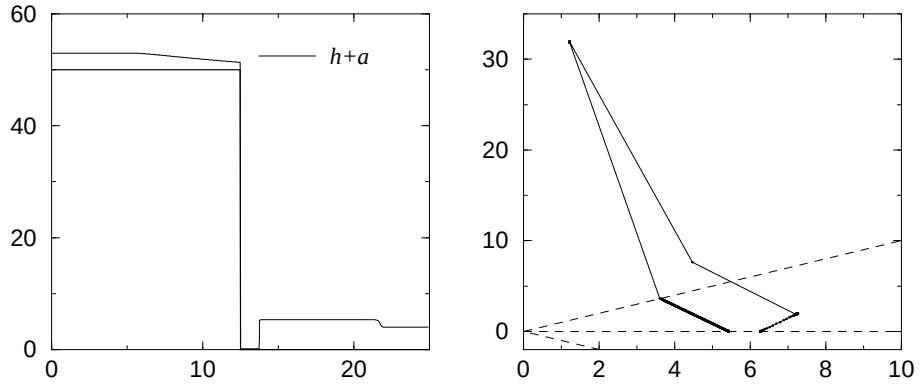

Figure 15: A test with a large decreasing jump of topography. Left: $h + a$ vs x. Right: u vs c.

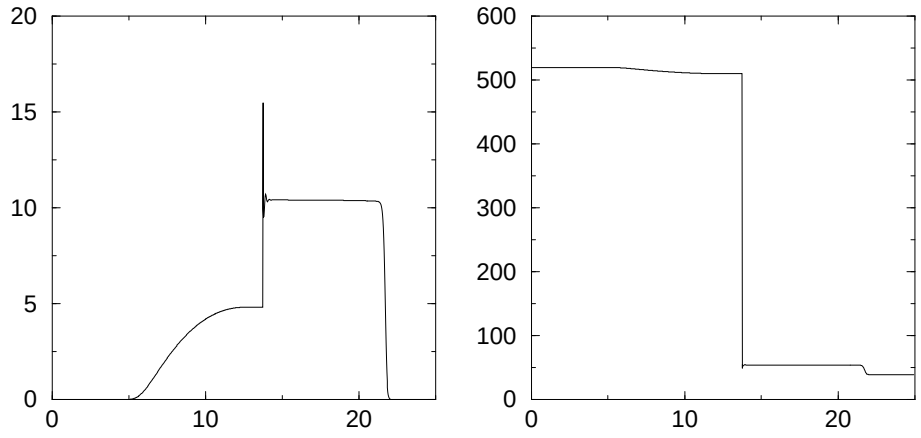

Figure 16: A test with a large decreasing jump of topography. Left: hu vs x. Right: $u^2/2 + g(h + a)$ vs x.

5 Conclusion

We have presented in this paper the well-balanced numerical scheme associated to the shallow-water equations with topography. This numerical scheme is based on the Riemann problem associated with this system and, due to the jump of topography, the model becomes nonstrictly hyperbolic. The solution of the Riemann problem is no longer classical [GL03], the uniqueness is lost for some initial data and we provide several guidelines for the construction of a solution. In particular, we prove that the states on each side of the jump of topography belong to the same critical mode (that is $\mathcal{F}$ or $\mathcal{T}$) in the non resonant case. In the case of resonance phenomenon, we have shown that the states on each side of the jump of topography can belong to different critical modes. It means that in the case of a decreasing topography which we focus on, a fluvial mode can become a torrential mode through a stationary shock (hydraulic jump) and the Bernouilli's law can be violated.

After having exhibited several Riemann solutions, we have presented the numerical approximations associated with these solutions, showing that the well-balanced numerical scheme computations are in a very good agreement with the previous analysis. Indeed, even with a large jump of topography, the method provides stable and accurate results.

This numerical scheme has also been implemented in the two-dimensional code Rozavel, which uses structured hexagonal meshes [Seg99]. Moreover, the extension of the well-balanced numerical scheme to the shallow-water equations with a source term of friction is also under investigation, based on [CL99].

References

[AR97] M. Amora and P. L. Roe, On post-shock oscillations due to shock capturing schemes in unsteady flows, *J. Comp. Phys.*, 1997, vol. 130-1, pp. 25–40.

[AW04] N. Andrianov and G. Warnecke, On the solution to the Riemann problem for the compressible duct flow, accepted in *SIAM J. Appl. Math*, 2004. Available at http://www.math.ntnu.no/conservation.

[Bou02] F. Bouchut, An introduction to finite volume methods for hyperbolic systems of conservation laws with source, In *École CEA-EDF-INRIA – Écoulements peu profonds à surface libre, Free surface geophysical flows*, INRIA Rocquencourt (France), October 2002. Available at http://www.dma.ens.fr/∼fbouchut/publications/fvcours.ps.gz.

[CL99] A. Chinnayya and A.-Y. LeRoux, *A new general Riemann solver for the shallow-water equations with friction and topography*, 1999. Available at http://www.math.ntnu.no/conservation.

[Col92] J.-F. Colombeau, *Multiplication of distributions*, Springer Verlag, 1992.

[CP98] F. Coquel and B. Perthame, Relaxation of energy and approximate riemann solvers for general pressure lawsin fluid dynamics, *SIAM J. Numer. Anal.*, Vol. 26-4, pp. 2223–2249, 1998.

[DLM95] G. Dal Maso,P. G. LeFloch and F. Murat, Definition and weak stability of non conservative products, *J. Math. Pures Appl.*, Vol. 74, pp. 483-548, 1995.

[dSV71] A. J. C. de Saint-Venant, Théorie du mouvement non-permanent des eaux, avec application aux crues des rivières et à l'introduction des marées dans leur lit, *C. R. Acad. Sci. Paris*, 1871, vol. 73, pp. 147–154.

[EGH00] R. Eymard, T. Gallouët, and R. Herbin, Finite Volume Methods, In *Handbook of Numerical Analysis* (Vol. VII), P. G. Ciarlet and J.-L. Lions Eds., North-Holland, pp. 713–1020, 2000.

[GHS03] T. Gallouët, J.-M. Hérard, and N. Seguin, Some approximate Godunov schemes to compute shallow-water equations with topography, *Computers and Fluids*, 2003, vol. 32-4, pp. 479–513.

[GL96a] L. Gosse and A.-Y. LeRoux, A well balanced scheme designed for inhomogeneous scalar conservation laws, *C. R. Acad. Sci. Paris*, 1996, vol. I-323, pp. 543–546.

[GL96b] J. M. Greenberg and A.-Y. LeRoux, A well balanced scheme for the numerical processing of source terms in hyperbolic equation, *SIAM J. Numer. Anal.*, 1996, vol. 33-1, pp. 1–16.

[GL03] P. Goatin and P. G. LeFloch, The Riemann problem for a class of resonant hyperbolic systems of balance laws, *preprint*, 2003. Available at http://www.math.ntnu.no/conservation.

[God59] S. K. Godunov, Finite difference method for numerical computation of discontinous solution of the equations of fluid dynamics, *Mat. Sb.*, 1959, vol. 47, pp. 271–300.

[Gos98] L. Gosse, A priori error estimate for a well-balanced scheme for inhomogeneous scalar conservation laws, *C. R. Acad. Sci. Paris*, 1998, vol. I-327, pp. 467–472.

[GR96] E. Godlewski and P.-A. Raviart, *Numerical approximation of hyperbolic systems of conservation laws*, Springer Verlag, 1996.

[IT95] E. Isaacson and B. Temple, Convergence of the 2×2 Godunov method for a general resonant nonlinear balance law, *SIAM J. Applied Math.*, 1995, vol. 55-3, pp. 625–640.

[KL02] A. Kurganov and D. Levy, Central-upwind schemes for the Saint-Venant system, M^2AN, 2002, vol. 36-3, pp. 397–425.

[LT03] P. G. LeFloch and M. D. Thanh, The Riemann problem for fluid flows in a nozzle with discontinuous cross-section, *preprint*, 2003.

[LeF89] P. G. LeFloch, Shock waves for nonlinear hyperbolic systems in nonconscervative form, *IMA Preprint Series*, 593, 1989.

[LeR98] A.-Y. LeRoux, Discrétisation des termes sources raides dans les problèmes hyperboliques, In *École CEA-EDF-INRIA – Problèmes non linéaires appliqués, Systèmes hyperboliques : nouveaux schémas et nouvelles applications*, INRIA Rocquencourt (France), March 1998. Available at http://www-gm3.univ-mrs.fr/∼leroux/publications/ay.le_roux.html.

[LeV98] R. J. LeVeque, Balancing source terms and flux gradients in high-resolution Godunov methods: the quasi-steady wave-propagation algorithm, *J. Comp. Phys.*, 1998, vol. 146, pp. 346–365.

[PS01] B. Perthame and C. Simeoni, A kinetic scheme for the Saint-Venant system with a source term, *Calcolo*, 2001, vol. 38-4, pp. 201–231.

[Seg99] N. Seguin, *Génération et validation de Rozavel, un code équilibre en hydraulique 2D.* Mémoire de D.E.A., GRAMM, Université Bordeaux I, 1999. Available, in French, at http://www-gm3.univ-mrs.fr/∼leroux/publications/n.seguin.html.

[Sto92] J. J. Stoker, *Water waves*, New York, John Wiley & Sons Inc., 1992, *Wiley Classics Library*, xxvi+567p. The mathematical theory with applications, Reprint of the 1957 original, A Wiley-Interscience Publication.

[SV03] N. Seguin and J. Vovelle, Analysis and approximation of a scalar conservation law with a flux function with discontinuous coefficients, *Math. Mod. Meth. Appl. Sci. (M^3AS)*, 2003, vol. 13-2, pp. 221–250.

[Vas02] A. Vasseur, Well-posedness of scalar conservation laws with singular sources, *Methods Appl. Anal.*, 2002, vol. 9-2, pp. 291–312.

[Tad86] E. Tadmor, A minimum entropy principle in the gas dynamics equations, *Appl. Numer. Math.*, 1986, vol. 2, pp. 211–219.